

DRILLING SIMULATION AND USER PROGRAM FOR OIL AND GAS

I. WELL PLANNING

Amornthep Klayhan

A Thesis Submitted in Partial Fulfilment of the Requirements
for the Degree of Master of Science
The Petroleum and Petrochemical College, Chulalongkorn University
in Academic Partnership with
The University of Michigan, The University of Oklahoma,
Case Western Reserve University, and Institut Français du Pétrole
2014

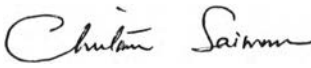
I28369671

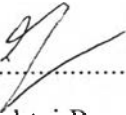
Thesis Title: Drilling Simulation and User Program for Oil and Gas
I. Well Planning
By: Amornthep Klayhan
Program: Petroleum Technology
Thesis Advisors: Assoc. Prof. Chintana Saiwan
Dr. Ruktai Prurapark

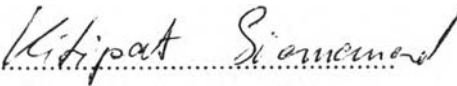
Accepted by The Petroleum and Petrochemical College, Chulalongkorn University, in partial fulfilment of the requirements for the Degree of Master of Science.



..... College Dean
(Asst. Prof. Pomthong Malakul)

Thesis Committee:


.....
(Assoc. Prof. Chintana Saiwan)


.....
(Dr. Ruktai Prurapark)


.....
(Asst. Kitipat Siemanond)


.....
(Dr. Panithita Vithayasricharoen)

ABSTRACT

5573001063: Petroleum Technology Program

Amornthep Klayhan: Drilling Simulation and User Program for Oil and Gas I. Well Planning.

Thesis Advisors: Assoc. Prof. Chintana Saiwan, and Dr. Ruktai Prurapark 112 pp.

Keywords: Torque/ Drag/ Well Planning/ Directional Drilling

Torque and drag (T&D) analysis is considered essentially in the well planning phase to ensure the efficient, economical, and safe planning, especially in directional drilling because drilling equipment can be damaged or buckled prior to reaching a target depth due to excessive T&D. The T&D analysis was performed using a soft-string model to develop software via the graphic user interface (GUI) of MATLAB. The software runs multiple scenarios of operation modes, rotating off-bottom, rotating on-bottom, pulling of the hole, and running into the hole. The well planning can be updated with new data to rapidly improve the operation efficiency. Furthermore, it can be applied to almost all wellbore types, such as build, hold, drop, and horizontal. The well trajectory model can be illustrated in three-dimension. The normal contact force, axial force, buckling and torque can be presented in graphical form. Additionally, the effect of weight on bit (WOB), density of drilling fluid (DF), and heavy weight drill pipe (HWDP) on T&D values at the surface were investigated by the software. The increase in WOB increases the axial force and torque at the surface as the same as the direction of the HWDPs placed. While the axial tension force was increased due to the increase of MW, the torque of rotating on-bottom at the surface was decreased. These effects will also help avoid the buckling problem. The software was also evaluated T&D values using the actual field data in Thailand with the reasonably accurate prediction.

บทคัดย่อ

อมรเทพ คล้ายหาญ : การวิเคราะห์การขุดเจาะและโปรแกรมสำหรับผู้ใช้ด้านน้ำมัน และแก๊ส ส่วนที่ I การวางแผนการขุดเจาะ (Drilling Simulation and User Program for Oil and Gas I. Well Planning) อ. ที่ปรึกษา : รศ. ดร. จินตนา สายวรรณ และ ดร. รักไทย บุรพ์ภาค 112 หน้า

การวิเคราะห์แรงบิดและแรงต้าน (torque and drag analysis) มีความสำคัญในขั้นกระบวนการวางแผนการขุดเจาะ เพื่อคำนึงถึงประสิทธิภาพ ความคุ้มค่าทางเศรษฐศาสตร์และอันตรายที่อาจเกิดขึ้นในขณะการดำเนินการขุดเจาะ โดยเฉพาะอย่างยิ่งการขุดเจาะหลุมแบบเอียง เนื่องด้วยอุปกรณ์ที่ใช้ทำการขุดเจาะอาจได้รับความเสียหายหรือการโก่งงอของท่อเจาะ (buckling) ก่อนถึงจุดหมายที่ต้องการอันเนื่องมาจากการได้รับแรงบิดหรือแรงต้านเกินพิกัดความสามารถ การวิเคราะห์แรงบิดและแรงต้านดังกล่าวใช้แบบจำลองท่ออ่อน (soft-string model) เป็นพื้นฐานในการพัฒนาโปรแกรมผ่านการแสดงผลของผู้ใช้ภายใต้โปรแกรม MATLAB โปรแกรมดังกล่าวสามารถทำการวิเคราะห์กิจกรรมในการขุดเจาะทั้งการหมุนแบบไม่สัมผัสปลายหลุม (rotating off-bottom) การหมุนแบบสัมผัสปลายหลุม (rotating on-bottom) การดึงขึ้น และการลงไปในหลุมของท่อขุดเจาะซึ่งสามารถวิเคราะห์ได้ทุกรูปแบบของหลุม เช่น แนวตรง แนวโค้ง แม้กระทั่งแนวราบ โดยรูปแบบหลุมแสดงออกในรูปแบบสามมิติ และผลจากการวิเคราะห์แรงบิดและแรงต้าน รวมทั้งแรงตั้งฉากการสัมผัสและแรงกดอัดที่สามารถเกิดอันตรายแสดงอยู่ในรูปแบบแผนภูมิที่แสดงความสัมพันธ์ของค่าดังกล่าวกับระยะในแนวตามท่อขุดเจาะ นอกจากนี้การศึกษาผลของน้ำหนักที่ให้กับหัวเจาะ (weight on bit) ความหนาแน่นของน้ำโคลนช่วยขุดเจาะ (density of drilling fluid) และท่อเจาะชนิดหนักพิเศษ (heavy weight drillpipe) ต่อค่าแรงบิดและแรงต้านบนฐานขุดเจาะด้วยโปรแกรมที่พัฒนา พบว่าการเพิ่มน้ำหนักให้หัวเจาะทำให้เพิ่มแรงดึงและแรงบิดบนฐานขุดเจาะเพิ่มขึ้น ในทิศทางเดียวกับการใช้ท่อเจาะชนิดหนักพิเศษ ในขณะที่แรงดึงเพิ่มขึ้นเนื่องจากการเพิ่มความหนาแน่นของน้ำโคลน ส่วนแรงบิดของการหมุนบนปลายหลุมลดลง การศึกษาผลกระทบดังกล่าวจะช่วยในการป้องกันปัญหาการโก่งงอของท่อเจาะ อีกทั้งโปรแกรมสามารถประเมินผลเทียบกับหลุมตัวอย่างที่ทำการขุดเจาะจริงในประเทศไทยได้ผลลัพธ์ที่เหมาะสม

ACKNOWLEDGEMENTS

The author, Mr. Amornthep Klayhan is grateful for the scholarship and research funding provided by The Petroleum and Petrochemical College and The National Center of Excellence for Petroleum, Petrochemicals, and Advanced Materials, Thailand.

I would like to express my appreciation to my supervisor Assoc. Prof. Chintana Saiwan at the Petroleum and Petrochemical College, Chulalongkorn University, for her help throughout the entire research work and contributions during the first year student till the last year of my Master degree.

I would like to give a special thanks to Dr. Ruktai Prurapark for his supervision, advice, and guidance from the beginning of my study as well as giving me valuable experiences all the way through my research work, with his endurance and knowledge, while allowing me the opportunity to work independently.

My gratitude also extends to Asst. Kitipat Siemanond, and Dr. Panithita Vithayasricharoen for serving on my examination committee.

I am really thankful to all the people of PAN Orient Energy Siam (POES) for allowing me to have the first time of my work experience to access to the onshore rig site and to provide the actual field drilling data and geological data for my research. Without their help, this research would have less meaning.

Finally, I would like to thank my family, my colleagues, my friends, for their continuously support and inspiration throughout my entire studies.

TABLE OF CONTENTS

	PAGE
Title Page	i
Abstract (in English)	iii
Abstract (in Thai)	iv
Acknowledgements	v
Table of Contents	vi
List of Tables	iv
List of Figures	x
Abbreviations	xviii
List of Symbols	xx
CHAPTER	
I INTRODUCTION	1
II LITERATURE REVIEW	3
2.1 Drilling	3
2.1.1 The Fundamental Drilling Concept	3
2.1.2 Drilling Activities	4
2.1.3 Directional Drilling	5
2.2 Drilling Processes	8
2.3 Fundamental Concept of Torque and Drag	11
2.3.1 Torque	11
2.3.2 Drag	12
2.3.3 Normal force	14
2.3.4 Friction factor	15
2.3.5 Measurement of Torque and Drag	17
2.4 Torque and Drag Model	18
2.4.1 Soft String Model	18
2.4.2 Stiff String Model	19
2.4.3 Tortuosity Effect	20

CHAPTER	PAGE
2.4.4 Buckling	22
2.5 Torque and Drag Equation in Three-Dimensional Wellbore	23
2.5.1 Rotating Off Bottom (RoffB)	24
2.5.2 Pulling Out of the Hole (POOH)	29
2.5.3 Running into the Hole (RIH)	34
2.5.4 Rotating On Bottom (RonB)	38
2.6 Software Development	44
2.7 Numerical Method	47
2.7.1 Euler Method	47
2.7.2 Modified Euler Method or Euler Predictor-Corrector Method	47
2.7.3 Runge-Kutta Methods	48
III METHODOLOGY	50
3.1 Materials	50
3.1.1 Equipment	50
3.1.2 Software	50
3.2 Research Procedures	50
3.2.1 Initiation Stage	50
3.2.2 Preparation Stage	51
3.2.3 Execution and Control Stage	51
3.2.4 Closing Stage	54
IV RESULTS AND DISCUSSION	55
4.1 Well Planning User-Friendly Software	55
4.1.1 Introduction of the Software	55
4.1.2 Calculation of Solving Torque and Drag Equation	59
4.2 Actual Field Well	59
4.2.1 Well A	59

CHAPTER	PAGE
V CONCLUSIONS AND RECOMMENDATIONS	81
REFERENCES	83
APPENDICES	87
Appendix A Well A	87
Appendix B Field Experience	107
CURRICULUM VITAE	112

LIST OF TABLES

TABLE	PAGE	
2.1	Range of friction factors	16
4.1	Characterization of well trajectory in 3D and the input sign	57
4.2	Well description of well A as the inputs to the software	60
4.3	The drillpipe description of well A as the database of the software	60
4.4	Calculated torque of well A with various coefficient of frictions	64
4.5	Actual field torque and the calculated torque of well A at the surface	67
4.6	Actual axial force and the calculated axial force at the surface of well A	68
4.7	Actual field hookload and the calculated hookload of well A	70
4.8	Actual DF and the new DF of well A	75
4.9	Calculated axial force and torque at the surface of well A by various DF	76
4.10	Calculated axial force and torque at the surface of RonB of well A as the HWDP placed	78
A1	Definitive survey of well A	87
A2	Actual field data hookload (HK) and torque (T) of well A	91
A3	The bottom hole assembly (BHA) of well A	95
A4	The results of well trajectory of well A	96

LIST OF FIGURES

FIGURE	PAGE
2.1	Rotary drilling rig component. 3
2.2	Offshore casing design. 4
2.3	The trajectory of the directional well. 6
2.4	The real well trajectory. 7
2.5	A simple build/hold/drop well terminology. 7
2.6	Integrated pre well planning (IPWP) main phase's process. 10
2.7	Integrated pre well planning (IPWP) work flow. 10
2.8	Torque (T) to rotate the drillstring in the wellbore. 12
2.9	Normal (F_n) and axial (F_a) forces. 12
2.10	Drillstring section with the normal contact force. 14
2.11	Region of static friction and dynamic friction as a function of pulling force. 15
2.12	An overview of the hoisting system. 17
2.13	The top drive of a rig providing a torque to the drillstring. 18
2.14	Short elements in a drillstring. 19
2.15	Spiral borehole in 2D (Tracks 1 and 2) and 3D images. 21
2.16	The two-dimensional schematic of the drift equation. 21
2.17	Buckling: (a) sinusoidal buckling and (b) helical buckling. 22
2.18	Well geometry: (a) right turn (horizontal view), (b) drop-off section (vertical view), (c) build-up section (vertical view), and (d) left turn (horizontal view). 24
2.19	Illustration of differences between positive (downside) and negative (upside) normal contact forces in build section during RoffB. 25
2.20	Illustration of forces (axial force, F and normal contact force, N) in build section during RoffB. 26

LIST OF FIGURES

FIGURE	PAGE
2.21 Illustration of forces (axial force, F and normal contact force, N) in hold section during RoffB.	26
2.22 Illustration of differences between positive (downside) and negative (upside) normal contact forces in drop section during RoffB.	27
2.23 Illustration of forces (axial force, F and normal contact force, N) in drop section during RoffB.	28
2.24 Illustration of forces (axial force, F and normal contact force, N) when the wellbore turns right (horizontal view) during RoffB.	29
2.25 Illustration of forces (axial force, F and normal contact force, N) when the wellbore turns left (horizontal view) during RoffB.	29
2.26 Illustration of differences between positive (downside) and negative (upside) normal contact forces in build section during POOH.	30
2.27 Illustration of forces (axial force, F and normal contact force, N) in build section during POOH.	31
2.28 Illustration of forces (axial force, F and normal contact force, N) in hold section during POOH.	31
2.29 Illustration of differences between positive (downside) and negative (upside) normal contact forces in drop section during POOH.	32
2.30 Illustration of forces (axial force, F and normal contact force, N) in drop section during POOH.	33

LIST OF FIGURES

FIGURE	PAGE
2.31 Illustration of forces (axial force, F and normal contact force, N) when the wellbore turns right (horizontal view) during POOH.	34
2.32 Illustration of forces (axial force, F and normal contact force, N) when the wellbore turns left (horizontal view) during POOH.	34
2.33 Illustration of differences between positive (downside) and negative (upside) normal contact forces in build section during RIH.	35
2.34 Illustration of forces (axial force, F and normal contact force, N) in build section during RIH.	36
2.35 Illustration of forces (axial force, F and normal contact force, N) in hold section during RIH.	36
2.36 Illustration of differences between positive (downside) and negative (upside) normal contact forces in drop section during RIH.	37
2.37 Illustration of forces (axial force, F and normal contact force, N) in drop section during RIH.	38
2.38 Illustration of forces (axial force, F and normal contact force, N) when the wellbore turns right (horizontal view) during RIH.	39
2.39 Illustration of forces (axial force, F and normal contact force, N) when the wellbore turns left (horizontal view) during RIH.	39
2.40 Illustration of differences between positive (downside) and negative (upside) normal contact forces in build section during RonB.	40

LIST OF FIGURES

FIGURE	PAGE
2.41 Illustration of forces (axial force, F and normal contact force, N) in build section during RonB.	41
2.42 Illustration of forces (axial force, F and normal contact force, N) in hold section during RonB.	41
2.43 Illustration of differences between positive (downside) and negative (upside) normal contact forces in drop section during RonB.	43
2.44 Illustration of forces (axial force, F and normal contact force, N) in drop section during RonB.	43
2.45 Illustration of forces (axial force, F and normal contact force, N) when the wellbore turns right (horizontal view) during RonB.	44
2.46 Illustration of forces (axial force, F and normal contact force, N) when the wellbore turns left (horizontal view) during RonB.	45
2.47 Well planning and engineering flowchart.	46
2.48 Torque and drag analysis flowchart.	46
2.49 Schematic for modified Euler method.	48
3.1 User-friendly software consists of (a) input panel and (b) output panel.	52
3.2 The flow chart of the user-friendly software starting from the operation modes followed by the well types, and then the torque and drag calculations.	53

LIST OF FIGURES

FIGURE	PAGE
4.1	The developed of the user-friendly software. 55
4.2	Input panel of the user-friendly software consist of (a) well description, drillpipe, BHA; and (b) operation mode. 57
4.3	Output panels of the user-friendly software consist of (a) well trajectory in three dimensions, (b) the data of axial force, torque, and total measured depth at the rig floor, and (c) the graph of normal contact force, axial force, and torque versus measured depth. 58
4.4	Well Trajectory of well A (a) 3D view, (b) vertical view, and (c) horizontal view. 61
4.5	Calculated torque of RoffB of well A from the software at the coefficient of friction of 0.1 in each section. 63
4.6	Comparison of the RoffB and RonB of (a) the calculated torque and (b) the normal contact force of well A from the software at the coefficient of friction of 0.1. 65
4.7	Comparison of the normal contact force distributed along the drillstring of (a) RoffB and (b) RonB of well A from the software at the coefficient of friction of 0.1. 65
4.8	Comparison of the actual field torque of well A and the calculated torque at RoffB and RonB from the software with various coefficient of frictions from 0.1 to 0.4. 66
4.9	Comparison of the calculated axial force of well A with the from the software for coefficient of frictions (a) 0.1, (b) 0.2, (c) 0.3, and (d) 0.4. 68
4.10	Comparison of the actual field hookload of well A with the calculated axial force from the developed software for coefficient of frictions (a) 0.1, (b) 0.2, (c) 0.3, and (d) 0.4. 69

LIST OF FIGURES

FIGURE	PAGE
4.11 Comparison of the actual field hookload of well A with the calculated hookload from the software at the coefficient of friction of 0.3.	71
4.12 Calculated axial force and compressive buckling force of well A from the software at the coefficient of friction of 0.4.	72
4.13 Calculated axial force of RonB and compressive buckling force of well A from the software at the coefficient of friction of 0.3 by various WOB.	73
4.14 Calculated axial force of RonB and compressive buckling force of well A from the software at the coefficient of friction of 0.4 by various WOB.	73
4.15 Calculated torque of RonB of well A from the software at the coefficient of friction of 0.4 by various WOB.	74
4.16 Normal contact force of RonB of well A from the software at the coefficient of friction of 0.4 by various WOB.	75
4.17 Calculated axial force of RonB and compressive buckling force of well A from the software at the coefficient of friction of 0.4 by various DF.	76
4.18 Calculated torque of RonB of well A from the software at the coefficient of friction of 0.4 by various DF.	77
4.19 Calculated axial force of RonB and compressive buckling force of well A from the software at the coefficient of friction of 0.4 by HWDP placed in vertical section instead of DP.	78

LIST OF FIGURES

FIGURE	PAGE	
4.20	Calculated axial force of RonB and compressive buckling force of well A from the software at the coefficient of friction of 0.4 by HWDP placed in vertical and build section instead of DP.	79
4.21	Calculated axial force of RonB and compressive buckling force of well A from the software at the coefficient of friction of 0.4 by HWDP1 placed in vertical section and HWDP2 placed in vertical and build section.	79
4.22	Comparison of the torque of RonB of well A from the software by HWDP1 placed in vertical section and HWDP2 placed in vertical and build section.	80
A1	Normal contact force of different operations; (a) RoffB, (b) RonB, (c) POH, and (d) RIH at the FF of 0.1 of well A.	102
A2	Axial force of different operation at the FF of 0.1 of well A.	102
A3	Normal contact force of different operations; (a) RoffB, (b) RonB, (c) POH, and (d) RIH at the FF of 0.2 of well A.	103
A4	Axial force of different operation at the FF of 0.2 of well A.	103
A5	Normal contact force of different operations; (a) RoffB, (b) RonB, (c) POH, and (d) RIH at the FF of 0.3 of well A.	104
A6	Axial force of different operation at the FF of 0.3 of well A.	104
A7	Normal contact force of different operations; (a) RoffB, (b) RonB, (c) POH, and (d) RIH at the FF of 0.4 of well A.	105
A8	Axial force of different operation at the FF of 0.4 of well A.	105
A9	Axial force of RonB at the FF of 0.3 of well A at maximum WOB.	106
A10	Axial force of RonB at the FF of 0.4 of well A at maximum WOB.	106

LIST OF FIGURES

FIGURE		PAGE
B1	The on-shored rig.	108
B2	The on-shored rig floor and the hoisting component.	109
B3	The control panel of at the rig floor.	110
B4	The draw work of rig and dead line for indicating the hookload.	110
B5	The anchor of dead line for indicating the hookload.	111

ABBREVIATIONS

2D	Two-dimensional
3D	Three-dimensional
Az	Azimuth (degree)
BHA	Bottom hole assembly
BUR	Build rate (degree/100 ft)
BURLR	Left/right turn (degree/100 ft)
CHFF	Casing hole friction factor
CPU	Central processing unit
DLS	Dogleg severity (degree/30 ft)
DP	Drillpipe
ECD	Equivalent circulating density
ERD	Extended reach drilling
ERW	Extended reach wells
EOB	End of Build
FF	Coefficient of friction
GUI	Graphic user interface
HK	The hook load (lbf)
HWDP	Heavy weight drillpipe
ID	Inner diameter (inches)
Inc	Inclination (degree)
IPEP	Integrated pre well planning (Aldawood <i>et al.</i> , 2011)
KOP	Kick of point (ft)
MD	Measured depth (ft)
DF	Density of drilling fluid (lb/gal)
MWD	Measured while drilling
NPT	Non-productive time
OD	Outer diameter (inches)
ODEs	Ordinary differential equations
OHFF	Open hole friction factor

POH	Pulling out of the hole
RAM	Random-access memory
RIH	Running into the hole
RKB	Rotary kelly bushing
RoffB	Rotating-on bottom
RonB	Rotating-off bottom
ROP	Rate of penetration
RPM	Revolutions per minute
T	Torque (ft-lbf)
T&D	Torque and drag
TD	Total depth (ft)
TOB	Torque on bit (ft-lbf)
Top	Weight of the hoisting system (lbf)
TVD	True vertical depth (ft)
WOB	Weight on bit (lbf)

LIST OF SYMBOLS

θ, I	Inclination (degree)
ϕ	Azimuth (degree)
F_n	Normal contact force (lbf or lbf/ft)
F_a	Axial force (lbf/ft)
F_d	Drag force (lbf)
F_s, F_k	Static and kinetic or dynamic drag force (lbf)
W_e	Buoyed nominal weight (lb/ft)
β	Buoyancy factor
ρ_o, ρ_i	Density of fluid outside and inside of the drillpipe (lb/gal)
ρ_{pipe}	Density of drillpipe material (lb/gal)
A_o, A_i	Cross sectional area of outside and inside of the drillpipe (ft ²)
μ	Coefficient of friction or friction factor
μ_s, μ_k	Static and kinetic or dynamic coefficient of friction
V	Resultant speed
V_t	Trip speed
V_r	Angular speed
r_t	Radius about which rotation occurs
T_p	Planned tortuosity
T_l	Large scale tortuosity
T_m	Micro-tortuosity
T_{total}	Total tortuosity
D_{drift}	Average diameter in torque equations (inches)
D_{tj}	Diameter of tool joint (inches)
F_s	Sinusoidal buckling axial compressive force (lbf)
F_H	Helical buckling axial compressive force (lbf)
EI	Stiffness of the pipe
r_c	Radial clearance between the pipe and the wellbore (inches)
α	Angle used to calculate the deviation of the wellbore (radian)

N	Normal contact force (lbf/ft)
N_{turn}	Normal contact force while turning (lbf/ft)
$F(\alpha)$	Tensile force (lbf)
$F_c(\alpha)$	Compressive force (lbf)
R	Radius of curvature of the string element while the wellbore is in the build or the drop section (ft)
R_{turn}	Radius of curvature of the string element while the wellbore is turning (ft)
$T(\alpha)$	Torque (ft-lbf)
L_1	Length of hold section (ft)